

Electrical Property of Mo-Doped VO₂ Nanowire Array Film by Melting–Quenching Sol–Gel Method

L. Q. Mai,^{*,†,‡} B. Hu,[†] T. Hu,[†] W. Chen,^{*,†} and E. D. Gu[†]

*School of Materials Science and Engineering, Wuhan University of Technology, Wuhan, 430070, China,
School of Materials Science and Engineering, Georgia Institute of Technology, Atlanta, Georgia 30332-0245*

Received: July 6, 2006; In Final Form: August 21, 2006

Mo-doped VO₂ nanowire array film with good thermochromic properties was prepared by melting–quenching followed by heat treatment in a vacuum. The formation of the new microstructure is related to the cleavage of the oxide lamella along (001) and (100) plane with large interplanar spacing. Mo doping results in the loss of V⁴⁺–V⁴⁺ pairs and destabilizes the semiconductor phase and consequently lowers the semiconductor-to-metal transition temperature T_c from 64 to 42 °C. Because of enhancement of the electron concentration due to the presence of Mo donors, the Fermi level shifts toward the conduction band, resulting in the decrease of activation energy E_a , hence, temperature coefficient of resistance.

Introduction

Vanadium dioxide (VO₂) has attracted much attention because its semiconductor-to-metal (S–M) transition temperature (T_c) is near room temperature (68 °C), which makes it useful for application to electrical and optical switching devices.^{1–3} The properties of the phase transition of VO₂ films strongly depend on the nature of the crystal structure and their stoichiometry, including the film orientation and microstructure, oxygen content, and residual interface strain. To date, there have been various methods used for the successful deposition of VO₂ thin films such as chemical vapor deposition,⁴ reactive sputtering,⁵ laser ablation,⁶ and pulsed laser deposition.⁷ The sol–gel technique is known to be one of the most practical methods for coating large-area substrates.^{8,9} It is attractive to prepare VO₂ by the decomposition of V₂O₅ into 2VO₂ + 1/2O₂, but a rigid condition is necessary, i.e., an oxygen partial pressure of about 4×10^{-8} Pa at 527 °C or a temperature of about 1327 °C at standard pressure.¹⁰ Recently, one-dimensional (1D) nanostructures of vanadium oxides, such as nanowires,¹¹ nanorods,^{12,13} nanobelts,¹⁴ and nanotubes,^{3,15} are attracting much interest because of their high aspect ratio and easy diffusion path for carrier transport.¹⁶ In this letter, we prepare Mo-doped VO₂ nanowire array film under relatively mild conditions, i.e., a pressure of 1.0 Pa at 500 °C, by combining molten-quenching sol–gel techniques and heat decomposition in a vacuum. The introduction of Mo is to reduce the semiconductor-to-metal transition temperature.⁶

Experimental Section

The typical preparation process was as follows:¹⁷ V₂O₅ and MoO₃ powder were mixed in the molar ratio of 97:3 and molten

at 800 °C in a ceramic crucible. When the molten liquid was quickly poured into distilled water, a brownish V₂O₅ sol was formed. Gel-derived thin films were dip-coated on glass substrates from above sol with a withdrawal speed of 10 cm/min. Mo-doped thin films were obtained after thermal treatment under low vacuum (1.0 Pa) at 500 °C for 6 h (heating rate is 1.5 °C/min). For comparison, the undoped VO₂ film was prepared according to the same conditions. The structure of the products was characterized by a Shimadzu XD-3A X-ray diffraction (XRD) with graphite monochromatized Cu K α radiation ($\lambda = 0.15148$ nm) and nickel filter. Scanning electron microscopy (SEM) images were collected by employing the JSM-5610LV scanning electron microscope. Transmission electron microscopy (TEM) images were taken in a JEOL JEM-2010FEF microscope operated at 200 kV. The metal contents were determined by inductively coupled plasma–atomic emission spectroscopy (ICP–AES) on a PLASMA 300 apparatus, and its accuracy is $\pm 0.1\%$. The electrical switching property was measured by a HP-4294A apparatus using a two-probe method, and the heating and cooling rates of 2 °C/min were used.

Results and Discussion

The XRD pattern of undoped and Mo-doped VO₂ films is shown in Figure 1. It can be seen that the relative peak intensity of the diffraction planes (200) is much higher when compared with that of the undoped VO₂ film, thus showing highly oriented growth of Mo-doped VO₂ film. No other vanadium oxides are detected, indicating the main chemical composition of the thin film is homogeneous. The peaks are rather sharp, which indicated relatively high crystallinity. However, the peaks of MoO₃ are not also discovered in the XRD pattern of the sample, which is due to the fact that the MoO₃ forms a solid solution phase in the VO₂ thin film.

Examination by SEM and TEM (Figure 2) finds that the attained film is composed of the well-aligned, Mo-doped VO₂

* Corresponding authors. E-mail: lmai6@mail.gatech.edu and chenw@mail.whut.edu.cn.

[†] School of Materials Science and Engineering, Wuhan University of Technology.

[‡] School of Materials Science and Engineering, Georgia Institute of Technology.

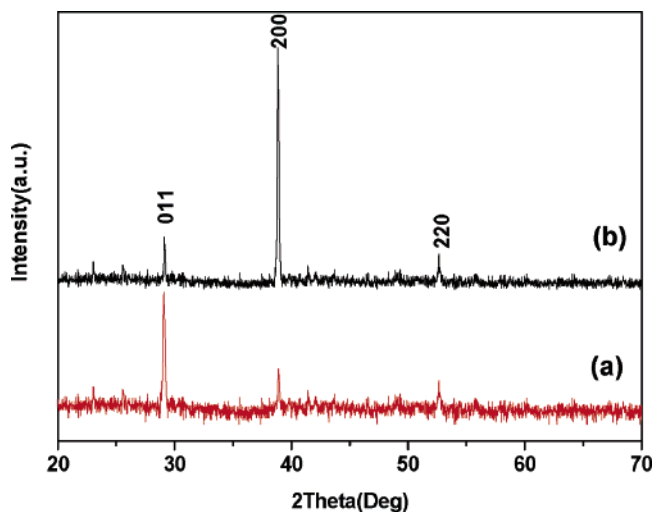


Figure 1. XRD pattern of undoped (a) and Mo-doped (b) VO_2 film.

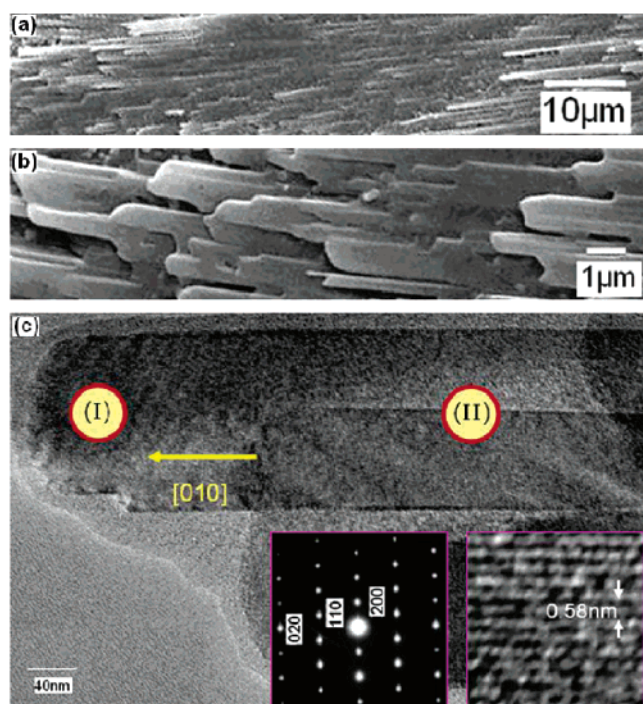
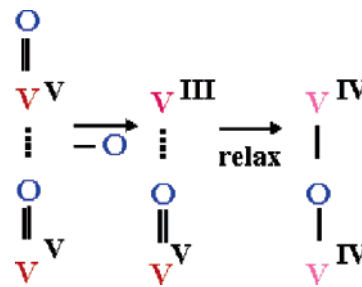


Figure 2. Low (a) and high (b) magnification SEM of Mo-doped VO_2 nanowire array film. (c) TEM image of a Mo-doped VO_2 nanowire. The left and right insets are the corresponding SAED and lattice fringe, respectively.

nanowires that are near parallel to the surface of glass substrate and show uniform morphology in 90% of the film area. VO_2 nanowires with a diameter of 80–600 nm and a length of 10–60 μm were formed (Figure 2a and b), which exhibits an interesting morphological feature: they are parallel to each other and indeed form bundles of agglomerated smaller filaments with diameters ranging from 40 to 60 nm (Figure 2c). The TEM image (Figure 2c) of a VO_2 nanowire and selected area electron diffraction (SAED) pattern (the left inset of Figure 2c) clearly demonstrate the single-crystalline nature of the grown nanowires with a [010] growth direction. The right inset of Figure 2c shows the clear lattice fringes with spacing of 0.58 nm between adjacent lattice planes corresponding to the distance between two (200) crystal planes of VO_2 . There are no visible defects or second phase in the Mo-doped VO_2 nanowire array. It means that the crystal lattice structure of the nanowires is fully formed, and the dopants are well integrated into the lattice sites and

result in the formation of a solid solution of $\text{V}_{0.97}\text{Mo}_{0.03}\text{O}_2$. The energy-dispersive X-ray spectra (EDS) from two different locations (I, II) along one VO_2 nanowire, as labeled in Figure 2c, were collected and the V and O signals of the nanowires as well as the Mo signal were observed along the entire length. Both the EDS spectra at locations I and II in VO_2 film show the atomic ratio of V and Mo are about 97:3. With consideration of the accuracy of the EDS microanalysis, we performed the ICP–AES analysis, and its result is $\text{V}_{0.971}\text{Mo}_{0.029}\text{O}_2$, which is in good agreement with the EDS results.

For the formation of Mo-doped VO_2 nanowire array, a probable process of the evolution of morphologies and crystal structures is as follows: (1) in the early drying process, the xerogel films (Figure 3, I) undergo a water evolution process from room temperature to about 300 $^\circ\text{C}$, and a crystallization process from 260 to 290 $^\circ\text{C}$. In this drying process, as most of the water is removed, the basal spacing of the layered structure is decreased to nearly a stable value and the Mo-doped vanadium oxide lamella (Figure 3a and II).¹⁸ (2) In the final vacuum heat treatment process in 500 $^\circ\text{C}$, the Mo-doped vanadium oxide lamella can be cleaved along the planes of (100) and (001) (Figure 3b and III) due to their large interplanar spacing, respectively, so Mo-doped VO_2 single-crystalline nanowire array (Figure 3c and IV) are formed. Notably, for the decomposition of V_2O_5 into $2\text{VO}_2 + \frac{1}{2}\text{O}_2$, a rigid condition is needed, i.e., an oxygen partial pressure of about 4×10^{-8} Pa at 527 $^\circ\text{C}$ or a temperature of about 1327 $^\circ\text{C}$ at standard pressure.¹⁰ However, in our work, under relatively mild conditions, i.e., a pressure of 1.0 Pa at 500 $^\circ\text{C}$, we prepared Mo-doped VO_2 nanowire array film. It is deduced that the formation of V_2O_5 gel films with higher reaction activity and introduction of Mo alter the reaction thermodynamics and the growth kinetics of VO_2 . In the vacuum heat treatment process at 500 $^\circ\text{C}$, the film experiences a reduction process with a release of O_2 . At the same time, the crystal structure will be adjusted to the final form as reduction occurs, which corresponds to a complicated process combined with oxygen release, crystal growth, and the formation of nanowire array by the cleavage along (001) and (100). The following is the schematic diagram of forming VO_2 from the V_2O_5 (001) surface:¹⁰



For comparison, the electrical resistivity (ρ) curves of undoped and Mo-doped VO_2 films versus temperature (T) are shown in Figure 4. The S–M transition temperature of the films T_c is defined as that corresponding to the peak in the curve obtained by plotting $d(\log \rho)/d(1/T)$ versus T , as shown in the inset of Figure 4b. The transition temperatures of the films are 64 $^\circ\text{C}$ for undoped and 41 $^\circ\text{C}$ for the Mo-doped films. The decrease of transition temperature has been witnessed previously in doped VO_2 films⁶ and can be attributed to the fact that the incorporation of Mo atoms leads to the loss of V^{4+} – V^{4+} pairs and destabilizes the semiconductor phase and consequently lowers the S–M transition temperature.¹⁹ The presence of molybdenum immediately narrows the hysteresis loop from 4

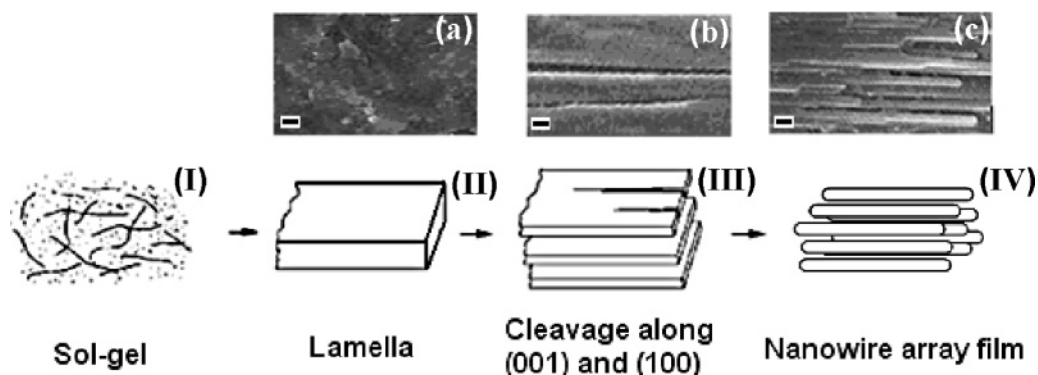


Figure 3. Schematic illustration of the evolution of Mo-doped VO₂ nanowire array. (a), (b), and (c) are the SEM images at corresponding stages. Scale bar 500 nm.

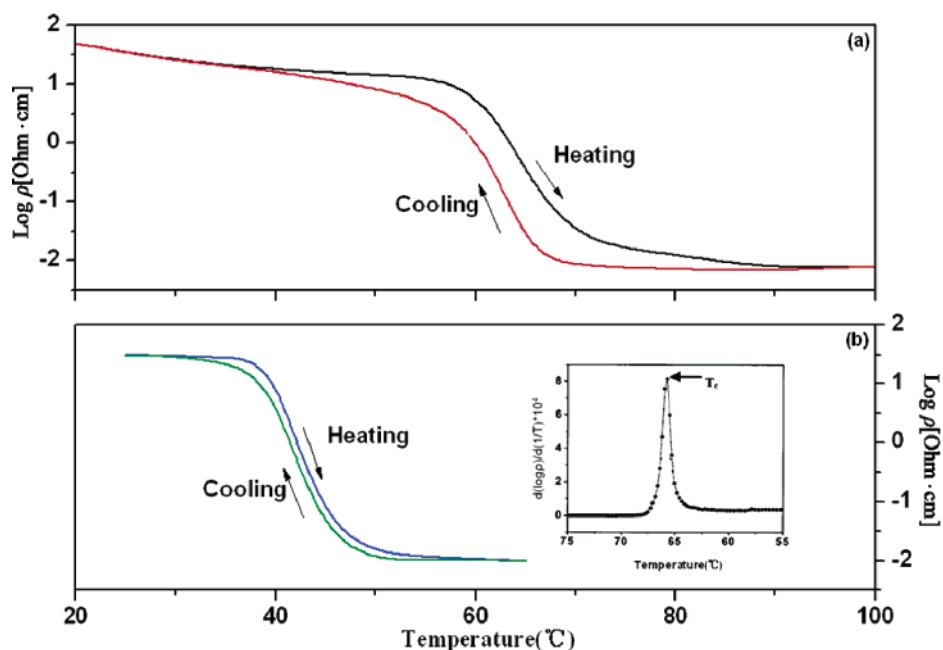


Figure 4. Temperature-dependent electrical resistivity curves of undoped (a) and Mo-doped (b) VO₂ films. The inset of (b) is the definition of transition temperature T_c .

°C for the undoped film to approximately 2 °C for Mo-doped film. The magnitude of the conductivity change across the transition decreased from 3.9 orders of magnitude for the undoped sample to 3.4 orders of magnitude for the Mo-doped film. This decrease can be explained by the higher conductivity of the semiconducting state of Mo-doped VO₂ films, which results from the enhancement of the carrier concentration due to the presence of Mo donors.

The electrical resistivity of the films in the semiconducting state, can be expressed as follows:

$$R_s = R_0 \times \exp[(E_c - E_f)/kT] \quad (1)$$

where E_c is the energy of the edge of the conduction band, E_f the Fermi level, k the Boltzmann constant, and R_0 the resistance at $T \rightarrow \infty$. The temperature coefficient of resistance (TCR) is defined as a slope parameter using the following equation:

$$\text{TCR} = \frac{1}{R_s} \times \frac{dR_s}{dT} \quad (2)$$

Combining eqs 1 and 2 yields

$$E_a = -kT^2 \times (\text{TCR}) \quad (3)$$

This relation links the activation energy $E_a = E_c - E_f$ to TCR. From the measured dependence of resistivity on temperature, we have determined E_a according to eq 2 and attained TCR from eq 3 (the TCR is nearly the same as the tested). The undoped VO₂ films are found to present a TCR of about $1.71 \pm 0.02\%/^{\circ}\text{C}$ and an E_a of about 0.143 ± 0.004 eV. However, a lower TCR of $1.38 \pm 0.02\%/^{\circ}\text{C}$ and an activation energy of 0.107 ± 0.004 eV are obtained for the Mo-doped VO₂ films. As we know, Mo doping increases the electron density in the film, which causes the Fermi energy level (E_f) shift toward the conduction band. As a result, E_a , hence TCR, decreases.

Conclusion

In conclusion, aligned nanowire film of Mo-doped VO₂ has been prepared by simple melting–quenching followed by heat treatment in a vacuum. The new microstructure is formed by the cleavage along (001) and (100) plane of the oxide lamella inherited from the layered structure of the vanadium oxide xerogel film. Mo-doped VO₂ nanowire array film shows a low S–M transition temperature of 42 °C and a narrow hysteresis loop of 2 °C. With the enhancement of the electron concentration due to the presence of Mo donors, the Fermi level shifts toward the conduction band, resulting in the decrease of E_a and then TCR.

Acknowledgment. Thanks to Prof. Z. L. Wang and Dr. R. S. Yang for help and many discussions. This work was supported by the National Natural Science Foundation of China (50372046), the Key Project of the Chinese Ministry of Education (104207), the Foundation for Innovation Research Team (2005ABC004) and the Natural Science Foundation (2006ABA310) of Hubei Province, Nippon Sheet Glass Foundation for Materials Science and Engineering (2005), the Teaching and Research Award Program for Outstanding Young Professors in Higher Education Institute, MOE, P. R. China, and the Wuhan Youth Chenguang Project (2006).

References and Notes

- (1) Muraoka, Y.; Hiroi, Z. *Appl. Phys. Lett.* **2002**, *80*, 583.
- (2) Aliev, R. A.; Klimov, V. A. *Phys. Solid State* **2004**, *46*, 532.
- (3) Mai, L. Q.; Chen, W.; Xu, Q.; Peng, J. F.; Zhu, Q. Y.; Yu, H. *Rare Metal Mater. Eng.* **2003**, *32*, 748.
- (4) Sahana, M. B.; Subbanna, G. N.; Shivashankar, S. A. *J. Appl. Phys.* **2002**, *92*, 6495.
- (5) Burkhardt, W.; Christmann, T.; Meyer, B. K.; Niessner, W.; Schalch, D.; Scharmann, A. *Thin Solid Films* **1999**, *345*, 229.
- (6) Wu, Z. P.; Miyashita, A.; Yamamoto, S.; Abe, H.; Nashiyama, I.; Narumi, K.; Naramoto, H. *J. Appl. Phys.* **1999**, *86*, 5311.
- (7) Soltani, M.; Chaker, M.; Haddad, E.; Kruzelecky, R. V.; Nikanpour, D. *J. Vac. Sci. Technol., A* **2004**, *22*, 859.
- (8) Verma, A.; Samanta, S. B.; Mehra, N. C.; Bakhshi, A. K.; Agnihotry, S. A. *Sol. Energy Mater. Sol. Cells* **2005**, *86*, 85.
- (9) Mackenzie, J. D.; Bescher, E. P. *J. Sol-Gel Sci. Technol.* **2000**, *19*, 23.
- (10) Ganduglia-Pirovano, M. V.; Sauer, J. *Phys. Rev. B* **2004**, *70*, 045422.
- (11) Chen, W.; Peng, J. F.; Mai, L. Q.; Xu, Q.; Zhu, Q. Y. *Chin. J. Inorg. Chem.* **2004**, *20*, 147.
- (12) Pinna, N.; U., W.; Urba, J.; Schlogl, R. *Adv. Mater.* **2003**, *15*, 329.
- (13) He, J. H.; Lao, C. S.; Chen, L. J.; Davidovic, D.; Wang, Z. L. *J. Am. Chem. Soc.* **2005**, *127*, 16376.
- (14) Liu, J. F.; Li, Q. H.; Wang, T. H.; Yu, D. P.; Li, Y. D. *Angew. Chem., Int. Ed.* **2004**, *43*, 5048.
- (15) Liu, X.; Taschner, C.; Leonhardt, A.; Rummeli, M. H.; Pichler, T.; Gemming, T.; Buchner, B.; Knupfer, M. *Phys. Rev. B* **2005**, *72*, 115407.
- (16) Dai, Z. R.; Pan, Z. W.; Wang, Z. L. *Adv. Funct. Mater.* **2003**, *13*, 9.
- (17) Chen, W.; Xu, Q.; Hu, Y. S.; Mai, L. Q.; Zhu, Q. Y. *J. Mater. Chem.* **2002**, *12*, 1926.
- (18) Livage, J.; Beteille, F.; Roux, C.; Chatry, M.; Davidson, P. *Acta Mater.* **1998**, *46*, 743.
- (19) Goodenough, J. B. *J. Solid State Chem.* **1971**, *3*, 490.